Application specific photonic integrated circuits through generic integration, a novel paradigm in photonics.

P. Muñoz[a,b], J.D. Doménech[a,b], I. Artundo[a,b], C. Habib[c], X.J.M. Leijtens[d], T. de Vries[d], D. Robbins[d], J. H. den Besten[b], L.R. Chen[c], and J. Capmany[a,b]
[a]Instituto de Telecomunicaciones y Aplicaciones Multimedia / [b]VLC Photonics S.L.
Edificio 8G – Acceso D – Planta 4 Universitat Politècnica de València
c/ Camino de Vera s/n – 46022 Valencia – Spain
Corresponding author: pascual.munoz@vlcphotonics.com
[c]Photonics Systems Group, Electrical & Computer Eng. Dept.
McGill University 3480 University St. Montreal, Quebec Canada H3A-2A7
[d]Opto-Electronic Devices group, COBRA Research Institute
TU Eindhoven P.O. Box 513 5600 MB Eindhoven, The Netherlands

Abstract

This paper reviews our recent work on integrating photonic devices and sub-systems onto a single photonic chip, by means of generic integration.

1. Introduction

Micro-electronic integrated circuits populate our world, both in industrial and in domestic applications: from the cell phone in our pocket, to the most sophisticated equipment in telecommunications, aeronautics, health-care, transportation and energy plants. The design and production of these micro-electronic circuits, known as Application Specific Integrated Circuits (ASICs), evolved from specialized art to mass technology during the last half of the past century. Their remarkable success lies in the existence of a few generic standard technologies to fabricate ASICs in a cost-effective way. This enables fab-less companies without having their own expensive fabrication capabilities to produce dedicated chips in large as well small quantities [1,2]. This model of generic standard technologies in electronics is currently being mirrored in opto-eletronics (or photonics). Photonic integrated circuits, also known as Application Specific Photonic Integrated Circuits (ASPICs) allow the production of components and sub-systems with the following characteristics: low cost, high energy efficiency, small footprint, high performance, high operation stability and multiple functionalities [3].

This paper is structured as follows: in section 2, a review on the state of the art of generic photonic integration technologies is presented. Following, in sections 3 and 4 our recent ASPIC developments on Silicon-On-Insulator and InP technologies are detailed. The conclusions are drawn on section 5.

2. Generic photonic integration technologies

ASPIC production has been done for years using vertical specialization or integration, with a model focused on the component. This model is based on the identification of needs for a certain device, as for instance a semiconductor laser for long reach communications. Then, to produce this very particular component, manufacturing machinery is acquired, a fabrication process is developed tailored to the development of that very precise component, and the overall will result in the best device according to the means available. On the other hand, generic integration focuses on the applications, which are the driving force towards the end components, which are in principle very different. Hence, a vertical fabrication process is not suitable to serve several applications. In contrast, a fabrication process is developed in which several building block devices, compared to the single specialized device mentioned above, can be produced. The number of combinations of these building blocks results in very different end devices for, in principle, very different applications. In this case the specialization is on the application, rather than on a single device, and this application specialization is enabled through the building blocks available in the generic integration fabrication process [1]. Generic integration opens the door to pure-play foundries, which are companies solely devoted to chip manufacturing, and also to design houses, which are companies without in-house chip fabrication facilities (fabless). This model is very well established in microelectronics, and was started in the mid 80s [2].

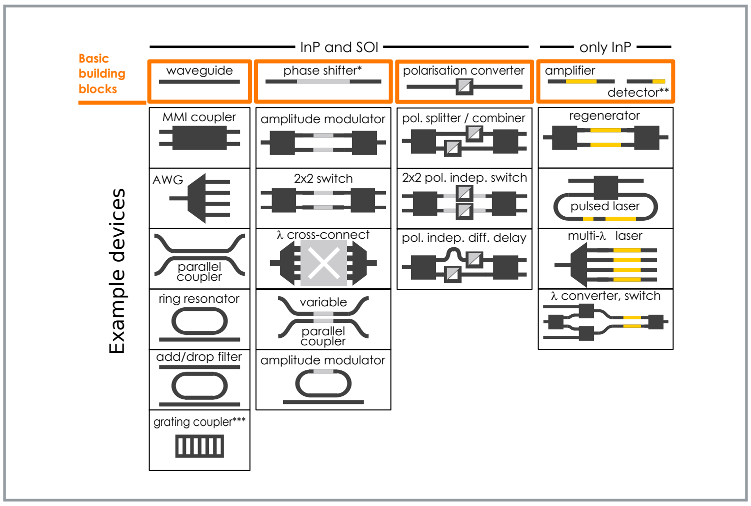

■ **Figure 1** *InP and SOI building blocks and example devices (adapted from Reference [12]). * Phase shifters in InP can use the thermo-optic and electro-optic effects, while in SOI only the thermo-optic. ** Detectors are also possible with SOI. *** Grating coupler can only be implemented in SOI.*

There are several photonic integration technologies. These technologies are based in different material systems, being the most relevant: Silicon based photonics (Silicon on Insulator [4] –SOI-, Silica on Silicon [5] -SiO2/Si- and Silicon Nitride[6] -Si3N4/SiO2-), III-V photonics [7] (Indium Phosphide –InP- and / or Gallium Arsenide –GaAs-) and Lithium Niobate [8] (LiNbO3). However, efforts to establish generic processes are mainly addressed towards SOI and InP photonics. Two clear examples of SOI generic foundry processes are ePIXfab at Europe [9] and OpSIS at the United States [10]. On the other hand, InP photonics generic foundry services is offered in Europe by JePPIX [11].

The capabilities of SOI and InP are described in the literature [4][12], and a graphical summary of the building blocks available is provided in Fig. 1.

3. Silicon photonics: box shaped optical filters

Coupled Resonator Optical Waveguides [13] (CROWs) are structures built with side coupled optical resonators, and their main application amongst others is as optical filters. CROWs can be built from building blocks as waveguides and couplers, from those of Fig. 1. Their spectral response can be tailored by the windowing or apodization of the inter-ring coupling coefficients in order to reduce the passband ripples.

Fig. 2-(a) shows the schematic of a CROW where the apodization has been done by changing the gap between resonators in order to change the coupling constant. For a fixed coupler length (L_c), the gaps are changed in steps that are of the order of nanometers. With this technique, good results can be achieved employing e-Beam lithography where small fields are written line by line (time consuming) with nanometric precision. On the other hand, for big scale production techniques as deep UV photolithography, where the complete circuit layout in a mask, compared to e-Beam writing, is revealed in a shot, the resolution decreases and therefore the small changes required for the apodization cannot be obtained by changing the gap between resonators. In Fig. 2-(b), the power coupling constant vs the coupler

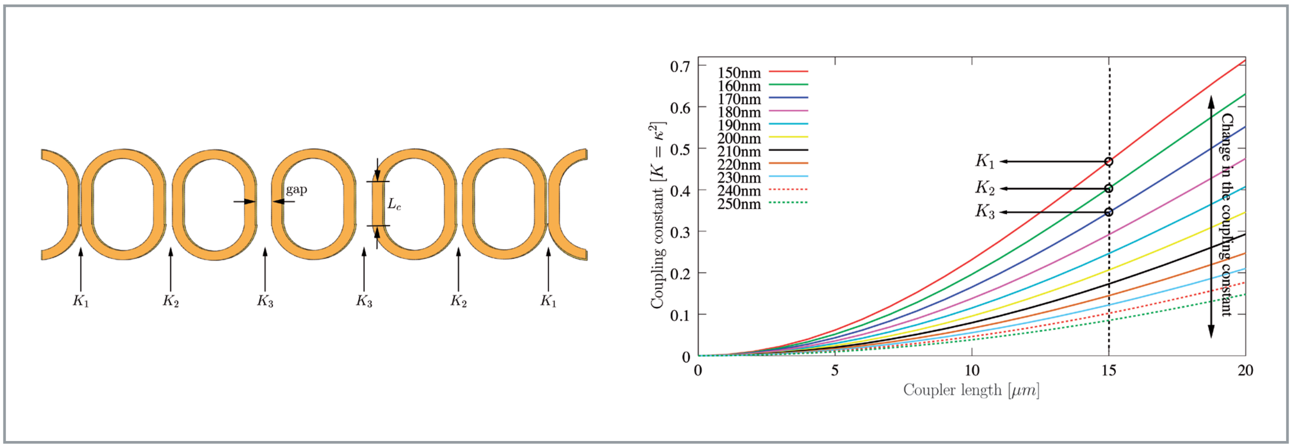

■ **Figure 2**. *Schematic drawing of gap apodization technique (a) and coupling constant variation vs. gap (b).*

ASPICs allow the production of component and sub-systems with the following characteristics: low cost, high energy efficiency, small footprint, high performance, high operation stability and multiple functionalities.

length (L_c) for several air gaps between cells of a CROW is plotted. In the case of the example of Fig. 2-(a), in order to achieve the desired coupling constant values for a fixed coupler length (K1,K2,K3), the variation of the gap should be as small as 50 nm, obtaining very different results if the nominal value of the gaps deviate from the desired just some nanometers as we have already demonstrated through simulation in [14].

With the longitudinal offset technique [14], the coupling constant value K is changed by imposing a longitudinal offset between the coupled waveguides. The offset, (L_{off}), shown in Fig. 3-(a), is imposed in the longitudinal direction, while the distance between the waveguides, gap, in the transversal direction is kept fixed in all the couplers of the CROW device. The offset implies a reduction in the coupler effective length. The technique allows for both increasing and decreasing the value of K starting from a nominal value. Fig. 4 shows again the coupling constant vs the coupler length for several air gaps for the proposed coupling scheme. Now the gap between cells is kept fixed (in this example 150 nm), and the coupling constant is set by applying a longitudinal offset of microns or hundreds of nanometers. A deviation in the gap will affect all the couplers at the same time, whilst a deviation in the offset values is two orders of magnitude less sensitive to changes affecting the coupling constants.

CROWs with 3 and 5 ring resonators were fabricated in the ePIXfab Silicon-On-Insulator platform [9] employing 193 nm deep UV photolithography processes, amenable for wafer scale mass production. The devices have been fabricated in a SOI wafer with a Silicon layer of 220 nm on top of a 2 μm Silicon Oxide BOX layer. The waveguides width for the straight and bent sections of the devices has been set to 450 nm leading to a group index of about 4.25 for wavelengths near 1.55 μm. The CROWs are based on racetrack shaped resonators with a bending radius of 5 microns and a straight coupling section of 53.3 μm. The first device is shown in the SEM image of Fig. 4-(a). It consists of 3 racetrack shaped resonators with a fixed spacing of 150 nm in the four couplers. The length of the straight coupling sections is fixed to 53.3 μm and the bending radii are set to 5 μm as mentioned previously. The coupling constants are designed to be equal in all the couplers with a nominal value of K = 0.25. Fig 4-(b) shows the transfer matrix method and the measured spectra. As expected, the spectra show ripples in the passband of about 5 dB. Predicted results and measurements are in good agreement. Fig. 4-(c) shows a SEM image of a 3 racetracks offset apodized CROW. In the case of the offset apodized device, the physical parameters (straight section length, bending radii, gaps) are kept constant, whilst a longitudinal offset is applied to the cavities. The first and the last resonator have the same offset and the central resonator has a smaller offset. The coupling constants are set to be 0.78, 0.33, 0.33 and 0.78 respectively. Again, as shown in Fig. 4-(d) the theoretical and measured responses are in good agreement, despite a small ripple in the left part of the passband.

The second kind of fabricated devices are 5th order filters with the same characteristics as the previous. The first one is an uniform filter with equal couplings constants K = 0.25 and a SEM image is shown in Fig. 5-(a). The measured repose is compared versus the simulated in Fig 5-(b). The asymmetry in the left part of the measured spectrum can be due to a combination of the CIFS effect [15], that is not taken into account in the transfer matrix model employed in the simulations, and a defect in the exposition of the lithographic process [4]. The last device shown in Fig. 5-(c) is a 5 rings offset apodized CROW. The coupling constants are defined to be 0.78, 0.56, 0.26, 0.26, 0.56 and 0.78 respectively. Again the measured an simulated responses are depicted in Fig. 5-(d) and as in the uniform case, the left part of the spectrum shows an asymmetry induced by the CIFS effect.

4. InP photonics: optical internet label swapper on a chip

One of the major drivers for a change from circuit to packet optical networks will be the availability

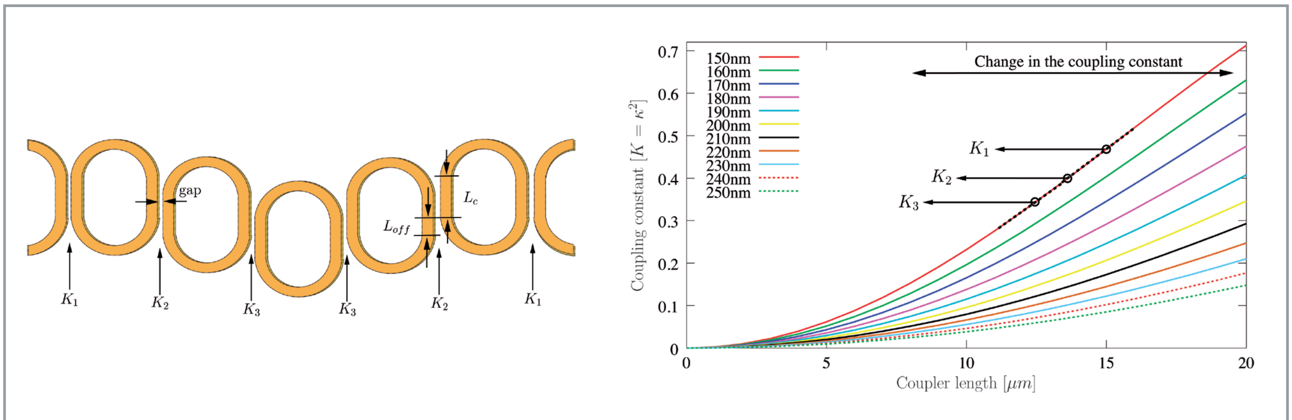

■ **Figure 3**. *Schematic drawing of longitudinal offset apodization technique (a) and coupling constant variation vs. offset length (b).*

of cheap and power efficient components, able to perform the different network functions over data packets. Amongst these functions, operations over the packet headers (labels) are crucial. One approach is optical code multiprotocol label switching (OC-MPLS). A simple but yet effective labeling approach is the Spectral Amplitude Coded (SAC) label swapping [16]: a spectral band is reserved for labels, and divided into N wavelength slots, therefore enabling 2^{N-1} labels. A key component in a OC-MPLS network node is the label swapper (LS), which strips the incoming label, attaches a new label, and reinserts it with the payload. Devices using cross-gain modulation (XGM) in ring cavities have previously been demonstrated with high extinction and contrast ratios [17]. In particular, a proof-of-concept tabletop (2x1 m^2) label swapper using a two stage XGM-based fiber-ring laser has been demonstrated in [18]. The main drawbacks of this device were cost and low operating frequency (80 kHz) due to a lengthy cavity (8.9 m).

The micrograph in Fig. 6-(a) shows a label swapper device based on a linear multi-wavelength laser configuration, built using several of the building blocks in Fig. 1, with Sagnac Loop Reflectors (SLR), an Arrayed Waveguide Grating (AWG) and SOAs on a single InP chip. The device footprint is 4.5 x 2 mm^2. The device is a linear laser between the SLRs enclosing SOA2-AWG-SOA L_i i=1...4, where the SOA2 acts a common cavity gain medium, and the AWG and SOA L_i combination enable the different output wavelengths/labels. The light is out-coupled from the laser cavity using a side diffraction order of the AWG ('FSR out coup' in the figure). The device design, fabrication and multi-wavelength operation details are fully described in [19]. An additional waveguide at the SOA L_i side is laid out as input for the incoming labels, through SOA_1 that can be used as booster amplifier. The label swapper device operation is as follows: referring to Fig. 6-(a), one output lasing wavelength is enabled by biasing SOA_2 and one of the L_i SOAs (dashed red line); next, an external laser signal with proper wavelength to reach SOA_2 through the AWG is used as input (dashed blue line); the SOAs biases are adjusted to allow switching on and off the laser by turning off and on the input wavelength, so the output label is an inverted version of the input. To test the device static and dynamic operation, the setup of Fig. 6-(b) was assembled. First, the static operation of the LS was measured using a CW input signal from a TL, set at 1561.5 nm to reach SOA_2 through the AWG. Befote the LS, and the VOA set to 0 dB, the power was 20 dBm. Lensed fibers were used to couple in/out to/from the chip. The static operation curves, Fig. 7, correspond to the estimated on chip input and output power, at the points marked in Fig. 6-(a). The estimation was obtained through measurements of the propagation (5 dB/cm) and in/out coupling losses (5 dB), using auxiliary test structures. To measure the AWG losses the SOA_1 was not biased, and a value of 8 dB was obtained (5 dB insertion losses, 3 dB side order out coupling). Afterwards, spectrum traces were recorded with an OSA at the output, for different input powers tuned using the VOA. The peak power within 0.1 nm was

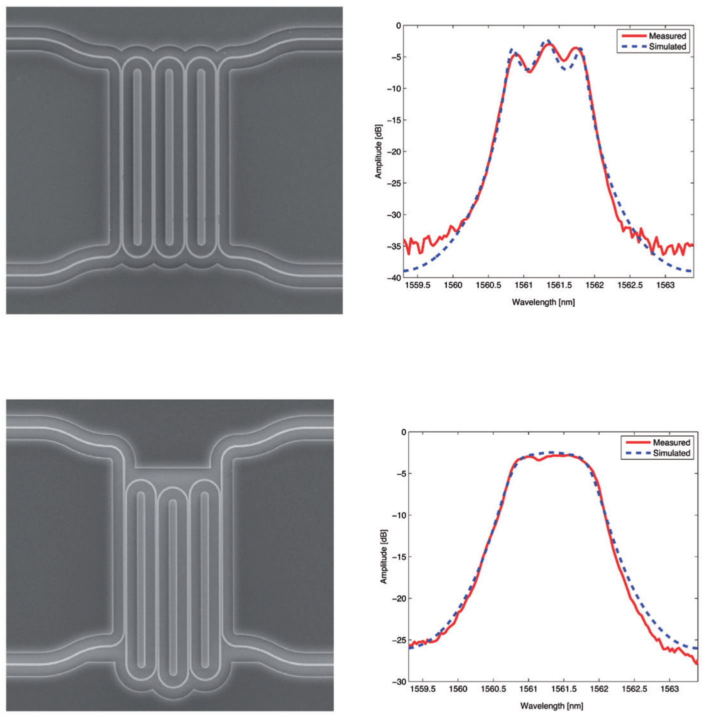

■ **Figure 4**. *SEM micrograph of uniform CROW (a) and simulated –dashed- and measured spectra –solid- (b) with 3 rings. SEM image for a 3 ring CROW (c) and simulated –solid- and measured spectra –dashed- (d).*

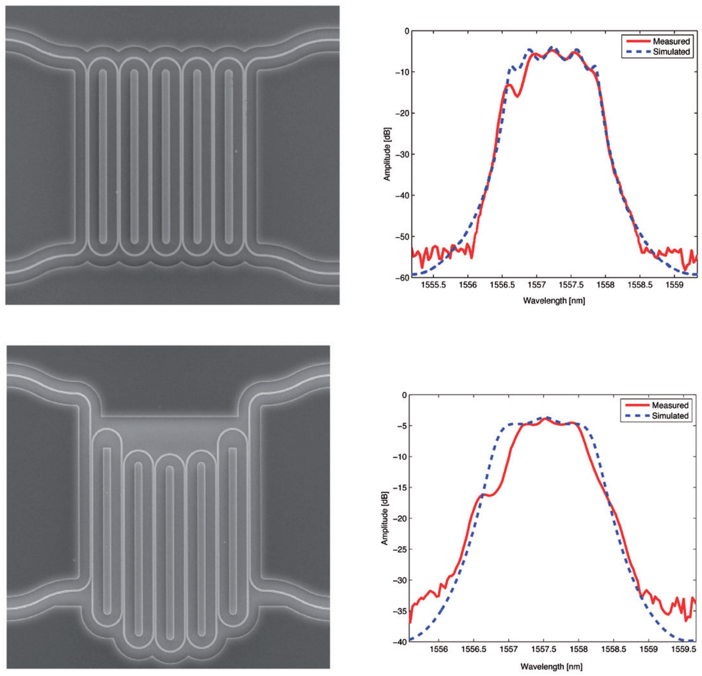

■ **Figure 5.** *SEM micrograph of uniform CROW (a) and simulated –dashed- and measured spectra –solid- (b) with 5 rings. SEM image for a 5 ring CROW (c) and simulated –solid- and measured spectra –dashed- (d).*

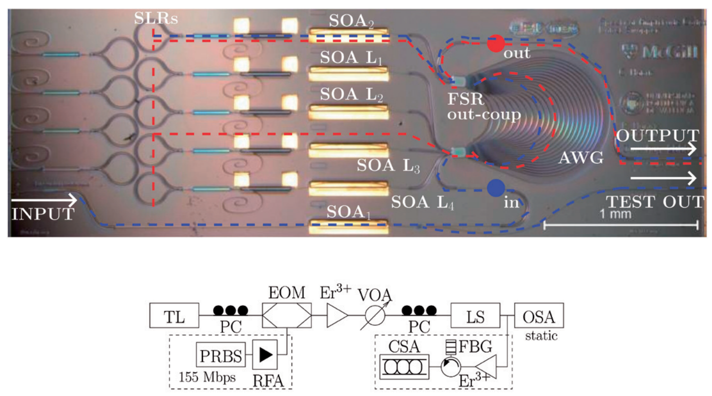

■ **Figure 6.** *Device micro graph, input, output and SOA's labeled (a) and characterization setup (b) (TL Tunable Laser, PC Polarization Controller, EOM Electro- Optic Modulator, RFA Radio-Frequency Amplifier, PRBS Pseudo Random Bit Sequence generator, Er3+ Erbium doped fiber amplifier, VOA Variable Optical Attenuator, LS Label Swapper chip, OSA Optical Spectrum Analyzer, FBG Fiber Bragg Grating, CSA Communications Signal Analyzer).*

recorded for the input and output (L4 1563.25 nm and L3 1564.81 nm) wavelengths. The laser operation with L1 and L2 exhibited mode hopping to side AWG resonances (FSR 8.1 nm). The static results shown in Fig. 2 are labeled as 'S-L4' and 'S-L3'. The contrast ratios are 28 dB and 33 dB respectively, and the on-off happens within an input power range of approximately 10 dB in both cases. Second, the dynamic operation of the device was assessed, using the setup in Fig. 6-(b) where the hardware enclosed in dashed lines was added. A PRBS generator operating at 155 Mbps followed by an RFA were used to drive the EOM. The output wavelengths were amplified, and subsequently filtered with a circulator and a FBG. In Fig. 7, a set of points labeled 'D-L4' and 'D-L3' overlay the static curves, corresponding to average input powers for which dynamic measurements were performed. The dynamic

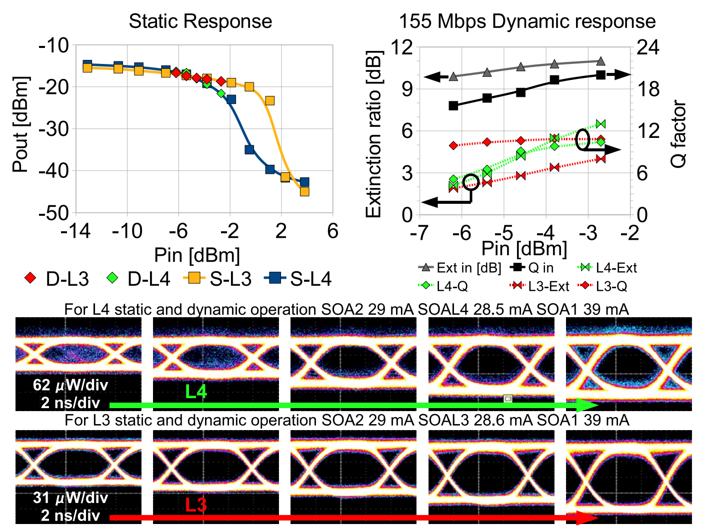

■ **Figure 7.** *Static operation (left) and dynamic(right) operation results.*

metrics, extinction ratio and Q factor, where acquired with a CSA, and are compared to the equivalent input power extinction ratio and Q factor measured back-to-back. The results are shown in the right panel of Fig. 7. The eye patterns for both output wavelengths are also shown at the bottom of the figure. In both cases the extinction ratio and Q factor trends agree with the static behavior. The rise and fall times, which correspond to the turn on and turn off times for the integrated laser, support the operation at 155 Mbps. The kHz limited operation in [3] was due to the long turn on and turn off times of the laser long cavity. The integrated LS provides shorter turn on/off times and avoids using guard bit slots, needed otherwise to prevent data loss.

Significant extinction ratio and Q factor penalties, right panel of Fig. 7, occur due to the fact the device is operated near threshold, but this can be overcome with post-amplification, as in the experiments. The differences between L4 and L3 operation in the extinction ratio and Q factor arise from the different slope in the static curves. Although the extinction ratio is always higher for L4, because the operation points are inside the static curve on-off transition, the Q factor is always higher for L3, for which the operation is always started from the unsaturated 'on' side. This is in agreement with the eye patterns shown in the figure (note the different vertical µW/div) where cleaner patterns occur for L3, with wider eyes (note the same horizontal scale in the graphs, 2 ns/div). A close look to the patterns also reveals slight differences between the rise (input fall) and fall (input rise) behavior in all the cases. The former corresponds to SOA slow recovery from carrier depletion, whilst the latter is due to fast dynamics. Hence, the traces are wider during the output rise than during the fall.

Compared to previous discrete component assembly implementations based on XGM switched lasers, the device is 10^5 smaller and operates 10^3 faster.

5. Conclusions

In this paper we have reviewed our recent activities in the development of ASPICs. Firstly, an overview of photonic generic integration technologies was presented, with special focus on the mainstream technologies SOI and InP. Using the available building blocks in these technologies, two of our recent ASPIC developments have been described. An optical filter in SOI technology, for which a special shaping technique amenable for large series production using photolithography has been presented. An optically switchable multi-wavelength laser ASPIC, of use in label swapping networks, developed in InP technology has also been introduced. Both examples are relevant samples of the potentials of generic integration photonic technologies.

Acknowledgements

This work has been partially funded through the Spanish Plan Nacional de I+D+i 2008-2011 project "Coupled Resonator Optical Waveguide eNgineering (CROWN)" grant no. TEC2008-06145/TEC, by the Generalitat Valenciana through project PROMETEO/2008/092 and by the EC FP6 contract no. 004525 ePIXnet. J.D. Doménech acknowledges the FPI research grant BES-2009-018381.

References

[1] J.T. Macher and D.C. Mowery, "Vertical specialization and industry structure in high technology industries," Advances in Strategic Management, vol. 21, pp. 317-356, 2004.

[2] C. Brown and G. Linden, "Offshoring in the Semiconductor Industry: A Historical Perspective," in 2005 Brookings Trade Forum on Offshoring of White-Collar Work.

[3] "Towards a foundry model in micro- and nanophotonics A vision for Europe," the ePIXnet (European Network of Excellence on Photonic Integrated Circuits and Components www.epixnet.org) Steering Committee, 2007.

[4] W. Bogaerts e.a., "Nanophotonic waveguides in silicon-on-insulator fabricated with CMOS technology," , Journal of Lightwave Technology, vol.23, no.1, pp. 401- 412, Jan. 2005.

[5] C.R. Doerr and K. Okamoto, "Advances in Silica Planar Lightwave Circuits," Journal of Lightwave Technology, vol.24, no.12, pp.4763-4789, Dec. 2006.

[6] F. Morichetti e.a., "Box-Shaped Dielectric Waveguides: A New Concept in Integrated Optics?," Journal of Lightwave Technology, vol.25, no.9, pp.2579-2589, Sept. 2007.

[7] E.A.J.M. Bente and M.K. Smit, "Ultrafast InP optical integrated circuits", in Proc. SPIE 6124, 612419, 2006.

[8] W. Sohler e.a., "Integrated Optical Devices in Lithium Niobate," Optics & Photonics News 19(1), 24-31 (2008).

[9] ePIXfab, The Silicon Photonics Platform, www.epixfab.eu

[10] OpSIS, Optoelectronic System Integration in Silicon, depts.washington.edu/uwopsis/

[11] JePPIX, Joint European Platform for InP-based Photonic Integrated Components and Circuits, www.jeppix.eu

[12] X.J.M. Leijtens, "JePPIX: the platform for InP-based photonics," in Proc. of the 15th European Conference in Integrated Optics (ECIO), pp. ThG3-1/2, Cambridge, United Kingdom, April 2010.

[13] A. Yariv, Y. Xu, R. K. Lee, and A. Scherer, "Coupled-resonator optical waveguide: a proposal and analysis," Opt. Lett. 24(11), pp. 711–713, 1999.

[14] J. Domenech, P. Muñoz, and J. Capmany, "The longitudinal offset technique for apodization of coupled resonator optical waveguide devices: concept and fabrication tolerance analysis," Opt. Express 17(23), pp. 21050–21059, 2009.

[15] M. Popovic, C. Manolatou, andM.Watts, "Coupling-induced resonance frequency shifts in coupled dielectric multi-cavity filters," Opt. Express 14(3), pp. 1208–1222, 2006.

[16] P. Seddighian, J. Rosas-Fernández, S. Ayotte, L. Rusch, S. Larochelle, and A. Leon-Garcia, "Low-cost scalable optical packet switching networks with multi-wavelength labels," in Proc. OFC/NFOEC, 2007, p. OthF5.

[17] R. Gordon and L. Chen, "Demonstration of all-photonic spectral label switching for optical MPLS networks," IEEE Photon. Technol. Lett., vol. 18, no. 4, pp. 586–588, 2006.

[18] C. Habib, V. Baby, L. Chen, A. Delisle-Simard, and S. Larochelle, "All-optical swapping of spectral amplitude code labels using non-linear media and semiconductor fiber ring lasers," IEEE J. Sel. Topics Quantum Electron., vol. 14, no. 3, pp. 879–888, 2008.

[19] P. Munoz, R. García-Olcina, J. Doménech, J. Capmany, L. Chen, C. Habib, X. Leijtens, T. de Vries, M. Heck, L. Augustin, R. Notzel, and D. Robbins, "Multi-wavelength laser based on an arrayed waveguide grating and sagnac loop reflectors monolithically integrated on InP," in Proc. ECIO, 2010.

Biographies

Pascual Muñoz

Pascual Muñoz obtained the M.Sc. degree in Telecommunication Engineering from Universitat Politécnica de Valencia (UPVLC) in 1998. After one year in the industry as IT Engineer, he returned to UPVLC to obtain his Ph.D degree in 2003, where he developed reference models for the design and modeling of integrated optics Arrayed Waveguide Grating (AWG) devices. The models were validated in collaboration with the company Alcatel Optronics (Livingston, UK). After his Ph.D. he moved to Technische Universiteit Eindhoven (TUe), where he was engaged on the design of AWG-based ASPICs for ultra-short pulses processing. Back into UPVLC, Pascual was appointed as coordinator for the "Joint Research Activity on InP AWG based devices" (2007-2009) in the ePIXnet network of excellence, where several research institutes and companies collaborated to develop multi-wavelength lasers for optical burst/packet switched networks. From 2008, Pascual was an Associate Professor at UPVLC.

Jan Hendrik den Besten

Jan Hendrik den Besten graduated in Physics and Dutch Literature at the University of Groningen in 1999 and received his Ph.D. degree from the Eindhoven University of Technology in 2004 for his work on the modelling and design, the technology and characterization of RF-modulators and multi-wavelength lasers in InP. From 2004-2006 he coordinated a "facility access activity" in the European "Network of Excellence" ePIXnet. In practice, this meant the coordination of researchers throughout Europe cooperating with researchers in Eindhoven in the development of various ASPICs. He helped shaping the "Joint European Platform for InP-based Photonic Integrated Components and Circuits" (JePPIX), about which he wrote an MBA-thesis (TiasNimbas Business School, 2006). From 2006-2011, he worked as development analyst and senior designer at ASML.

José Capmany

José Capmany obtained the M.Sc. degrees in Telecommunications Engineering and Physics from Universidad Politecnica de Madrid (UPM) and UNED respectively. He holds a Ph.D. in Telecommunications Engineering from UPM and a Ph.D. in Physics from the Universidad de Vigo. In 1991 he moved to the Universidad Politecnica de Valencia (UPVLC) where he has been a full Professor in Photonics and Optical Communications since 1996. In 2002 he was appointed Director of the Institute Of Telecommunications and Multimedia (iTEAM) at UPVLC. He has been engaged in many research areas within the field of photonics during the last 25 years including Microwave Photonics, Integrated Optics, Fiber Bragg Grating design and fabrication, Optical Networks and, most recently Quantum Information systems. He has published over 375 papers in scientific journals and confererences. He is a Fellow of the Institute of Electrical and Electronic Engineers (IEEE) and the Optical Society of America (OSA).

José David Doménech

J. D. Domenech received the B.Sc. degree in Telecommunications and the M.Sc. degree in Technologies, Systems and Networks of Communication from the Universidad Politecnica de Valencia (UPVLC) in 2006 and 2008 respectively. He is currently working towards the Ph.D. degree in optics at the Universidad Polit√©cnica de Valencia in the Optical and Quantum Communications Group and his research has been focused in the use of integrated ring resonators for microwave photonics applications. Since 2006, he has been working on the design of integrated optic circuits in Indium-Phosphide/Silicon Nitride/SOI technologies within several European and national research projects.

Íñigo Artundo

Íñigo Artundo obtained the M.Sc. in Telecom Engineering at the Universidad Pública de Navarra (Pamplona, Spain) in 2005, and received his Ph.D. in Applied Physics and Photonics at the Vrije Universiteit Brussel (Brussels, Belgium) in 2009. He has been involved in several European research projects and networks of excellence focused on optical interconnection networks, the fabrication and characterization of micro-optic devices and on flexible access and in-building fiber network architectures. He has worked as a reviewer for several scientific journals and national funding agencies. His main technical expertise is in board-to-board, chip-to-chip and on-chip optical links, and short-range dynamic optical communications.

Lawrence R. Chen

Lawrence R. Chen received the B.Eng. degree in electrical engineering and mathematics from McGill University in 1995 and the M.A.Sc. and Ph.D. in electrical and computer engineering in 1997 and 2000, respectively. Since 2000, he has been with the Department of Electrical and Computer Engineering at McGill University and is currently serving as Associate Dean for Academic Affairs in the Faculty of Engineering. In 2006-2007, he was on leave at Queen,Äôs University (Kingston, ON, Canada), Ryerson University (Toronto, ON, Canada), the Chinese University of Hong Kong (Hong Kong), and the Universidad Politecnica de Valencia (Valencia, Spain). His research interests are in ultrafast photonics and fiber optics and include all-optical signal processing, arbitrary waveform generation, fiber lasers and amplifiers, and fiber gratings. He has over 200 journal and conference publications. He is an Associate Editor (Canada) for the IEEE Photonics Society Newsletter, a Topical Editor for Optics Letters, and a member of the editorial advisory board for Optics Communications. He serves on the Board of Directors for the Centre d,Äôoptique, photonique et laser (COPL) in Quebec, Canada.